DOI: 10.1002/ejic.201000928

Coordination Chemistry of Thiazole-Based Ligands: New Complexes Generating 3D Hydrogen-Bonded Architectures

Andrea Rossin,[a] Barbara Di Credico,[a] Giuliano Giambastiani,[a] Luca Gonsalvi,[a] Maurizio Peruzzini,*[a] and Gianna Reginato[a]

Keywords: Heterocycles / Hydrogen bonds / Coordination modes / Supramolecular chemistry

The hydrothermal (solvothermal) reactions of Zn^{II}, Co^{II}, and Cu^{II} salts with the thiazole-based ligands 2-Htzc (thiazole-2-carboxylic acid), 4-Htzc (thiazole-4-carboxylic acid), and Htzc-py [2-(2-pyridyl)thiazole-4-carboxylic acid] led to the formation of coordination complexes with assorted geometry at the metal centers. The new complexes were characterized by conventional spectroscopic methods as well as by single-crystal X-ray analysis, TG–MS, and PXRD. Crystallographic studies have shown that an extended supramolecular network is generated in the solid state through the formaton of hydrogen bonds between the several polar groups present in the complex frameworks.

Introduction

The supramolecular assembly of organic, inorganic, and metal–organic species to create multidimensional well-defined architectures has become a very active area of research in the last 20 years, particularly after the discovery that the resulting materials have many specific practical applications.[1] Contemporary crystal engineering is full of examples of the self-assembly of discrete units sustained by hydrogen bonds or other weak interactions.[2] Hydrogen bonds are normally formed between polar functional groups and heteroatoms. Synthetic organic chemistry offers an extremely wide variety of accessible heterocycles, spanning the purely C,N-containing systems such as imidazoles, pyrazoles, triazoles, or tetrazoles to the "mixed" C,O/C,S-containing cycles such as furans, thiophenes, oxazoles, and thiazoles.[3] The solid-state aggregation of these species often leads to hydrogen-bonded architectures.[4] However, if this behavior is considered in the context of coordination chemistry instead, the simultaneous presence of both highly directional coordinative metal-to-ligand bonds and flexible complex-to-complex hydrogen bonds can generate virtually infinite multidimensional superstructures ranging from zero to three dimensions.[5]

We have recently turned our attention to the optimization of synthetic methodologies for the large-scale preparation of thiazole-based carboxylates.[6] Examples of thiazole-based spacers used for the synthesis of either multidimensional coordination polymers or organometallic complexes with a polymeric assembly in the solid state are still rather scant in the literature.[7] In crystal engineering, weak noncovalent interactions are of fundamental importance for the formation of highly ordered and possibly porous structures. The formation of a porous solid requires that the number of these weak interactions is high enough to compensate the energetic penalty for the existence of cavities in the crystal.[8] With this in mind we decided to investigate the coordination properties of thiazole-4-carboxylic acid (4-Htzc), thiazole-2-carboxylic acid (2-Htzc) and 2-(2-pyridyl)thiazole-4-carboxylic acid (Htzc-py, Scheme 1) towards different 3d metal salts such as zinc(II), cobalt(II), and copper(II).

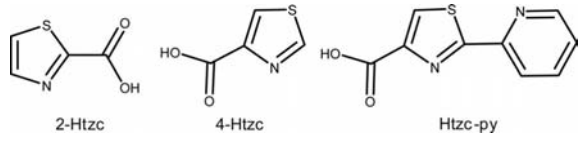

Scheme 1. Thiazole-based ligands used in this study.

Herein we present our results on the synthesis of a wide family of complexes that form supramolecular assemblies in the solid state, generating 3D hydrogen-bonded networks. Among them, an unusual trigonal-bipyramidal coordination geometry was found for the zinc(II) complex [Zn(tzc-py)$_2$(H_2O)] in which a metal-coordinated water molecule forms a quite unusual intramolecular hydrogen bond with the dangling *ortho*-pyridyl arm. This kind of arrangement is very uncommon for aromatic ligands.

[a] Consiglio Nazionale delle Ricerche, Istituto di Chimica dei Composti Organometallici (ICCOM-CNR),
Via Madonna del Piano 10, 50019 Sesto Fiorentino, Firenze, Italy
E-mail: maurizio.peruzzini@iccom.cnr.it

Supporting information for this article is available on the WWW under http://dx.doi.org/10.1002/ejic.201000928.

Results and Discussion

Ligand Thermal Stability and the Crystal Structure of 2-Htzc

Before preparing the metal–organic compounds, the thermal stabilities of the free ligands were examined by TGA–MS to assess the maximum temperatures at which the hydrothermal syntheses could be carried out without incurring undesired ligand decomposition. The TGA–DTG plot profiles of the three organic ligands used in this study are collected in Figure S1. Htzc-py is the most thermally robust ligand as its decomposition starts at over 221 °C with a peak temperature (T_P) at 243 °C (T_{onset} = 221.6 °C, T_{offset} = 255.7 °C) whereas 2-Htzc and 4-Htzc show maximum decomposition rates at 115 °C (T_{onset} = 96.8 °C, T_{offset} = 125.8 °C) and 215 °C (T_{onset} = 185.2 °C, T_{offset} = 217.2 °C), respectively. The MS spectra of the volatiles recorded during the heating of the three ligands evidence a peak corresponding to CO_2 production (m/z = 44) within the temperature ranges noted above. In all cases, the decarboxylation occurs almost simultaneously with the whole thermal decomposition of the samples, making any precise attribution of the weight loss impossible. The COOH group in the *ortho* position is the most labile, as confirmed by the general organic reactivity of substituted thiazoles,[9] and the acidic environment catalyzes the ligand decarboxylation (see below).

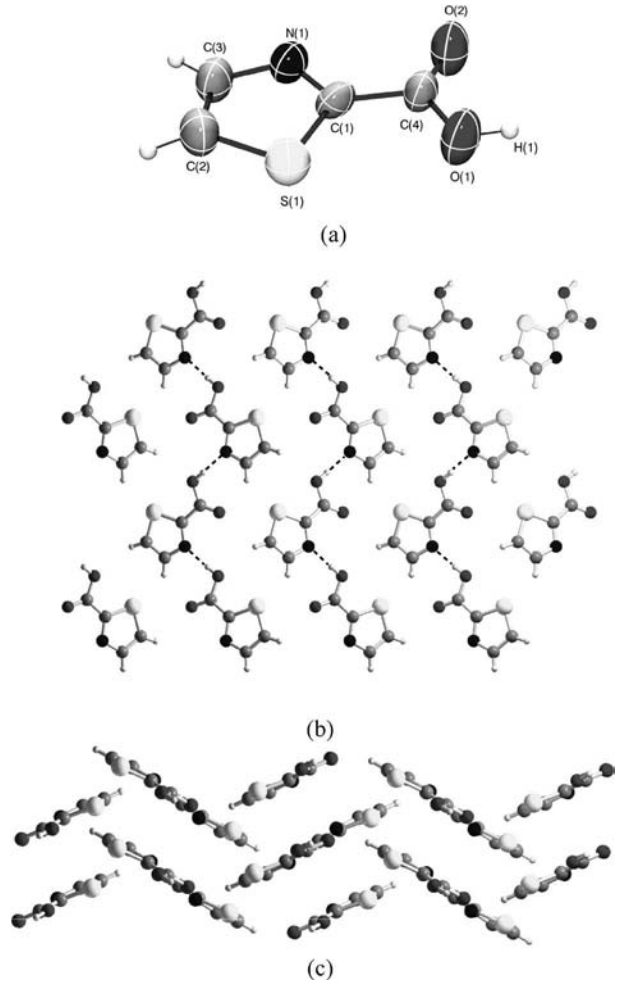

Figure 1. (a) Asymmetric unit of the crystal structure of 2-htzc (a). Views of its solid-state assembly along (b) the [001] and (c) the [010] Miller planes. Thermal ellipsoids in (a) are drawn at the 60% probability level. Hydrogen bonds in (b) are depicted as dotted lines.

Colorless prismatic crystals of 2-Htzc were obtained from concentrated acidic aqueous solutions upon cooling to +4 °C. The crystal structure of the ligand is shown in Figure 1. The main geometrical features of the heterocyclic ring are similar to those reported for the only other existing XRD structure of a thiazole-based molecule, Htzc-py.[6] Hydrogen-bonding between the OH moiety of the carboxylic group and the nitrogen atom of the adjacent thiazole ring in the lattice is present {*d*[O(1)···N(1)#] = 2.665(7) Å},[10] generating a zig-zag arrangement of the molecules in the crystal packing along the *c* axis that maximizes the number of these stabilizing interactions (Figure 1, b). Additional π-stacking between the aromatic rings can be observed [*d*(thiazole ring centroids) = 3.884 Å, with a slightly staggered relative disposition], generating an ordered assembly along the *b* axis as well (Figure 1, c). The overall "helicoidal" packing generates a noncentrosymmetric space group ($Pn2_1a$) with intrinsic chirality. See the Supporting Information (Tables S1 and S2) for the complete crystallographic data.

Synthesis of the Complexes and XRD Characterization: Towards Hydrogen-Bonded Architectures

To explore the coordination chemistry of the new thiazole-based ligands, the solvothermal synthetic technique was preferred a priori to the "classic" conditions (the reaction outcome being the same in both cases) for obtaining better crystals of the final products for the structural analysis. The solvothermal (hydrothermal) synthesis of coordination polymers is a well-known and widely applied technique.[11] Nonetheless, it is also applicable to the production of molecular species with a high degree of crystallinity in most cases. Unfortunately, there are many factors that control the final reaction outcome and the effect of each of them on the resulting material is as yet not clear.[12] The temperature, concentration, time, the nature of both the metal precursor and the counterion, and pH are all crucial in driving the reaction course.[13] In the reaction between the two regioisomeric forms of Htzc (thiazole-2- or -4-carboxylic acid) and zinc(II), two isomeric species of the same chemical formula $[Zn(tzc)_2]\cdot 2H_2O$ (**1** and **2**) were formed (Scheme 2).

The thermal lability of 2-Htzc above 100 °C rules out the possibility of carrying out the hydrothermal synthesis at higher temperatures. In addition, the decarboxylation process is ultimately favored by the strongly acidic conditions of the reaction medium; when zinc(II) chloride ($ZnCl_2$) was chosen as the metal precursor, under the same solvothermal conditions as described for **2**, the [$ZnCl_2$(κ-*N*-thiazole)$_2$] tetrahedral thiazole complex was finally isolated

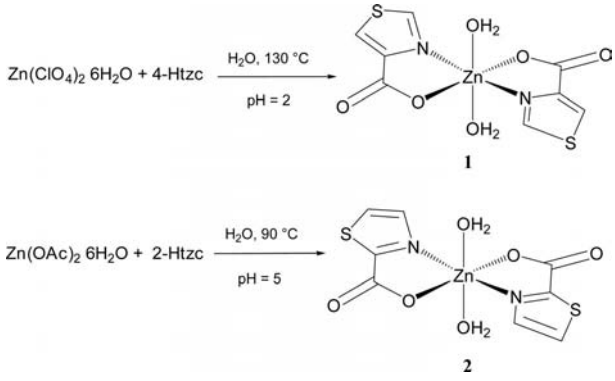

Scheme 2. pH- and temperature-dependent hydrothermal synthesis of **1** and **2**.

(see the Supporting Information for its XRD data).[14] This finding confirmed that the decarboxylation of 2-Htzc occurs at either $T > 100$ °C or pH ≤ 2. The hydrothermal reaction between copper(II) acetate and 2-Htzc at 90 °C did not lead to any ligand substitution: Crystals of the bis-hydrated metal precursor were collected, as confirmed by comparing the unit cell parameters of the isolated material with those of dimeric $[Cu_2(\mu\text{-}OAc)_2(H_2O)_2]$.[15] Although the final pH of the solution preserves the ligand from undesired decarboxylation, the stable acetate bridges in the Cu^{II} precursor do not allow for displacement by the 2-tzc$^-$ anion. The crystal structure of **1** is shown in Figure 2 (a). The zinc(II) cation is hexacoordinated in an octahedral geometry. The two aquo ligands are *trans* to each other in the axial positions and the two (deprotonated) 4-tzc ligands are *N*,*O*-chelating in a bidentate fashion in the equatorial plane, the zinc atom lying on an inversion center. The Zn–N(3) and Zn–O(1) bond lengths found in **1** (Tables S3 and S4) are similar to those reported for other zinc(II) complexes of the general formula $[Zn(L)_2(H_2O)_2]$ [L = 3-carboxy-1,2,4-triazole,[16] imidazole-4-carboxylate,[17] or 4-(carboxylato)-imidazole-5-carboxylic acid].[18] In these examples the imidazole- and triazole-based ligands have an identical κ^2-*N*,*O*-chelating coordination mode, the resulting complexes being isostructural with the thiazole-based analogue **1**. On the other hand, the Zn–N(3) distance is shorter than that observed in the complex (2,2′-diamino-4,4′-bi-1,3-thiazole)-bis(glycinato)zinc(II) [2.1823(13) Å],[19] and both the Zn–N and Zn–O bonds are longer than those found in the polymeric poly{aqua[4-(carboxylato)imidazole-5-carboxylic acid]zinc(II)} [1.985(2) and 2.020(3) Å, respectively].[18a] The supramolecular arrangement resulting from extensive intermolecular hydrogen-bonding between the coordinated water molecules and the carboxylic groups of adjacent molecules (Table 1) is similar to those seen in the aforementioned species.[20] This fact is responsible for the poor solubility of **1** in aqueous solutions.

A similar network featuring the same type of hydrogen-bonding pattern is observed in the isomeric complex **2** (Figure 3), the only difference being the position of the S atom in the heterocyclic ring. Neither new geometrical motifs nor other special solid-state properties are generated with respect to **1**. Tables S5 and S6 in the Supporting Information list the main structural parameters, the crystal data, and structure refinement details. The hydrogen-bonding pattern in the lattice is identical to that of **1** (Table 2).

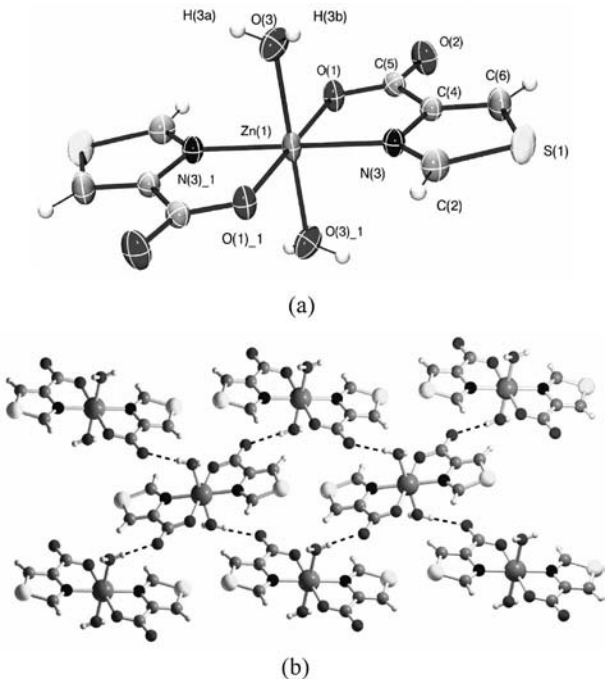

Figure 2. (a) Asymmetric unit of the crystal structure of **1**. (b) Views of its solid-state assembly along the [100] Miller planes. Thermal ellipsoids in (a) are drawn at the 60% probability level. Hydrogen bonds are depicted as dotted lines.

Table 1. Hydrogen bonds in **1**.

D–H···A[a]	*d*(D–H) [Å]	*d*(H···A) [Å]	*d*(D···A) [Å]	∠DHA [°]
O(3)–H(3a)···O(2)#2	0.76(4)	2.02(5)	2.779(3)	177(4)
O(3)–H(3b)···O(1)#3	0.82(5)	1.95(6)	2.769(3)	172(4)

[a] Symmetry transformations used to generate equivalent atoms; #2: $-x$, $y - ½$, $-z - ½$; #3: $x - 1$, y, z.

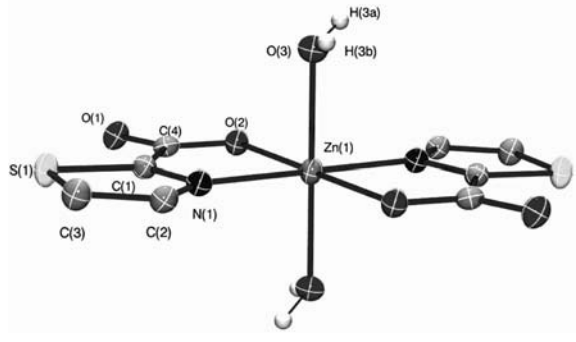

Figure 3. Asymmetric unit of the crystal structure of **2**. Thermal ellipsoids are drawn at the 60% probability level. Hydrogen atoms on C(2) and C(3) have been omitted for clarity.

The reaction of 4-Htzc with the copper(I) species $[Cu(MeCN)_4]PF_6$ in acetonitrile led to metal oxidation under aerobic conditions with the formation of the Cu^{II} complex

Table 2. Hydrogen bonds in **2**.

D–H···A[a]	*d*(D–H) [Å]	*d*(H···A) [Å]	*d*(D···A) [Å]	∠DHA [°]
O(3)–H(3a)···O(2)#2	0.86(3)	1.91(3)	2.740(3)	161(2)
O(3)–H(3b)···O(1)#3	0.76(3)	1.98(3)	2.725(3)	167(3)

[a] Symmetry transformations used to generate equivalent atoms; #2: $-x$, $y - ½$, $-z - ½$; #3: $x - 1$, y, z.

$[Cu(4\text{-tzc})_2]$ (**3**, Figure 4, a). The coordination geometry around the four-coordinate copper center is approximately square planar {∠[N(3)–Cu–O(1)] = 83.67(15)°, ∠[N(3)–Cu–O(1)#] = 96.33(15)°} and the metal atom lies on an inversion center (Tables S7 and S8). The tendency for Cu^{II} to attain an octahedral coordination geometry is evident by the short contacts present in the crystal structure {*d*[Cu–O(2)#] = 2.89 Å}. The copper coordination sphere is expanded by engaging in additional weak interactions with the O(2) oxygen atoms of the upper and lower lattice molecules to form a distorted octahedral geometry (Jahn–Teller elongation along the axial direction). As a result, the final assembly is a columnar arrangement of the molecules along the *a* axis with the molecules slightly staggered with respect to one another (Figure 4, b). Crystals of complex **3** are poorly soluble in water, like those of **1**, because the extensive number of such (weak) interactions overcome the solvation effects.

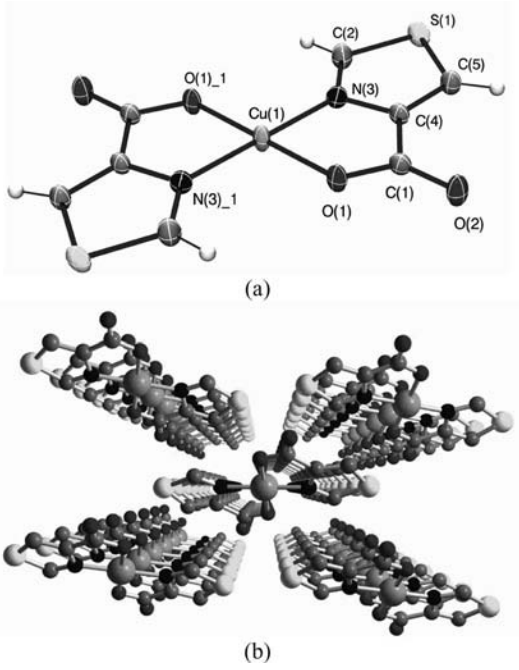

Figure 4. (a) Asymmetric unit of the crystal structure of **3**. (b) Views of its solid-state assembly along the [100] Miller planes, showing the pillared arrangement of the complex molecules in the lattice. Thermal ellipsoids in (a) are drawn at the 40% probability level.

The chemical versatility of the Htzc-py ligand is related to its pH-dependent protonation/deprotonation equilibria in water, which make this system very similar to a "classic" amino acid (Scheme 3).

Indeed, the simultaneous presence of an acidic and a basic site within the same molecule makes Htzc-py very interesting from a supramolecular point of view, engaging in multiple coordination modes. The regioisomer of Htzc-py containing a *para*-pyridyl substituent in the 2-position [2-(4-pyridyl)thiazole-4-carboxylic acid, pytac], has already been investigated and found capable of generating 3D coordination polymers with silver(I),[7e] zinc(II),[7e] and copper(II).[7f] The other regioisomer bearing a *meta*-pyridyl dangling ring also forms polymeric species with zinc(II), cobalt(II), and copper(II).[7d] In the case of Htzc-py, the N atom of the *ortho*-pyridyl group cannot form bridges between two metal centers because it is constrained geometrically. As a result, discrete complexes are formed (Scheme 4) in which the *ortho*-pyridyl substituent (either protonated or deprotonated) is involved in intramolecular hydrogen-bonding.

The "zwitterionic" form of tzc-Hpy is the one that appears in the crystal structure of **4** (Figure 5, a): The zinc atom is hexacoordinated with the ligand occupying the equatorial plane and displaying the same κ^2-*N*,*O* coordination mode as 4-Htzc in complex **1**. The metal lies on a crystallographic inversion center and two water molecules *trans* to each other complete the octahedral coordination geometry (Tables S9 and S10). The strongly acidic pH environment (the perchlorate anion does not alter the initial pH conditions) generates a protonated nitrogen atom on the pyridyl substituent, thus, the "pyridinium-like" ring is in-

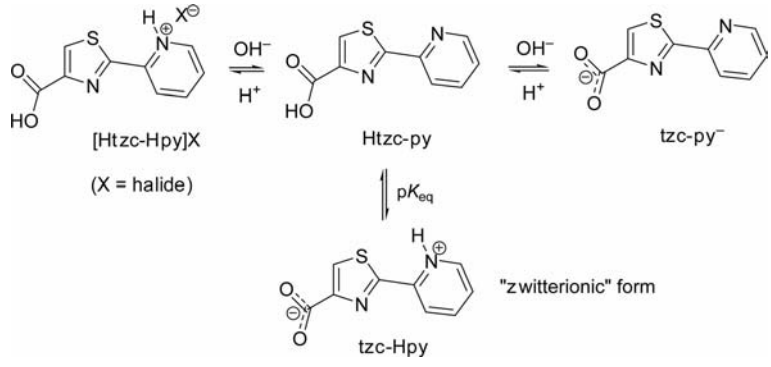

Scheme 3. Protonation/deprotonation equilibria of Htzc-py in water.

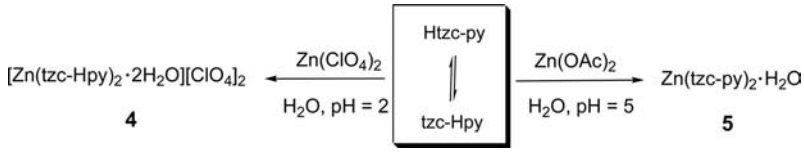

Scheme 4. Reactivity of Htzc-py with zinc(II) salts.

volved in a N(2)–H(2)···O(2)# hydrogen bond. Additional interactions between the aquo ligands and the C=O groups of neighboring molecules [O(1)–H(1a)···O(3)#] and between the same ligands and the (disordered) perchlorate ions [O(1)–H(1b)···$OClO_3$] are present (Table 3). The final result is a complex network of embedded hydrogen bonds that holds all the components together in a compact assembly (Figure 5, b). The θ[N(1)–C(1)–C(5)–N(2)] dihedral angle is very small [4.3(8)°] with the pyridyl ring almost coplanar with the thiazole ring.

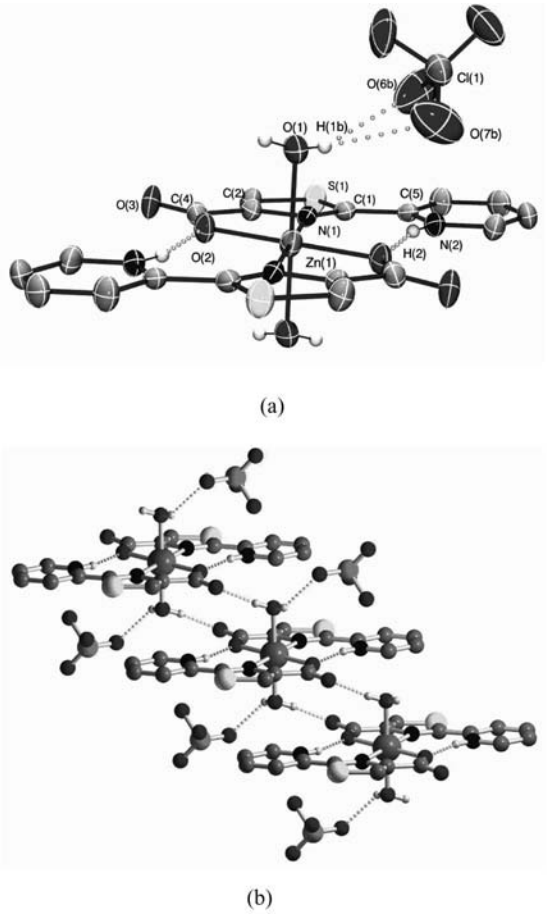

Figure 5. (a) Part of the asymmetric unit of **4**. (b) View of the complex hydrogen-bonding network present in the lattice. Hydrogen atoms not relevant to the discussion have been omitted for clarity. Thermal ellipsoids in (a) are drawn at the 40% probability level. Disorder at perchlorate O(6) and O(7) are not explicitly drawn.

The two nitrogen atoms N(pyridyl) and N(thiazole) are in a cisoid conformation, whereas the opposite situation is observed in the free Htzc-py ligand [θ = 179.8(8)°].[6] The

Table 3. Hydrogen bonds in **4**.

D–H···A[a]	*d*(D–H) [Å]	*d*(H···A) [Å]	*d*(D···A) [Å]	∠DHA [°]
O(1)–H(1a)···O(3)#2	0.82	1.84	2.647(5)	169.4
O(1)–H(1b)···O(5a)	0.75	2.21	2.777(14)	133.1
O(1)–H(1b)···O(7b)	0.75	2.47	3.051(15)	135.5
N(2)–H(2)···O(2)#1	0.86	1.89	2.737(6)	166.0

[a] Symmetry transformations used to generate equivalent atoms; #1: $-x + 1, -y + 1, -z + 1$; #2: $-x, -y + 1, -z + 1$.

Zn–O(2) distance is shorter [2.001(4) vs. 2.1273(18) Å] and the Zn–N(1) is longer [2.242(4) vs. 2.066(2) Å] than the corresponding values found for **1**.

Under less acidic pH conditions, obtained by slow acetate hydrolysis in the presence of Htzc-py, a different coordination compound is obtained. The five-coordinate species **5** exhibits a distorted trigonal-bipyramidal geometry (Figure 6) with the deprotonated (tzc-py^-) ligand in the usual κ^2-*N*,*O* coordination mode. The N(thiazole) and O atoms occupy the axial and equatorial positions, respectively (Tables S11 and S12). The coordination polyhedron is completed by a water molecule located in the equatorial plane of the bipyramid. The pyridyl substituent of one ligand engages in one intramolecular hydrogen bond with the coordinated water molecule [O(5)–H(5a)···N(2)]. The two aromatic rings in this ligand are slightly twisted around the C–C linking bond: The θ[N(2)–C(3)–C(5)–N(1)] dihedral angle is 15.3(2)° with the pyridyl ring in a (distorted) cisoid conformation to allow for its interaction with water. The other ligand has the same conformation as the free Htzc-py ligand[6] with a transoid N(pyridyl)···N(thiazole) conformation {θ[N(3)–C(12)–C(14)–N(4) = 178.76(15)°]}. Finally,

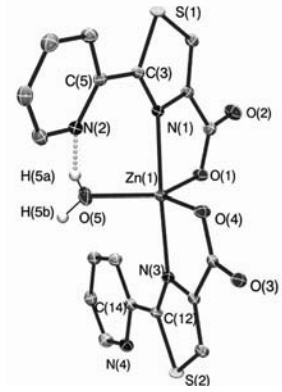

Figure 6. Crystal structure of complex **5**. Hydrogen atoms on the organic ligands have been omitted for clarity. Thermal ellipsoids are drawn at the 40% probability level.

the other hydrogen atom of the water ligand interacts with the carboxylic group of the neighboring molecule [O(5)–H(5b)···O(3)#, Table 4].

Table 4. Hydrogen bonds in **5**.

D–H···A[a]	*d*(D–H) [Å]	*d*(H···A) [Å]	*d*(D···A) [Å]	∠DHA [°]
O(5)–H(5a)···N(2)	0.84	1.86	2.664(2)	161.0
O(5)–H(5b)···O(3)#1	0.86	1.76	2.6153(2)	179.5

[a] Symmetry transformation used to generate equivalent atoms; #1: $x - 1$, y, z.

Although the Zn^{II} ion in its d^{10} valence electron configuration has no ligand field stabilization energy and can adopt many different coordination numbers (between four and eight), the trigonal-bipyramidal geometry is not a common leitmotiv in its coordination chemistry; scattered examples exist that contain tripodal ligands that "force" this geometrical arrangement due to their flexible aliphatic arms bearing pendant donor groups. Some of these ligands are the tetradentate ligands 2,2′,2′′-nitrilotriacetate (nta),[21] (2-picolyl)(*N*-pyrrolidinylethyl)(2-hydroxy-3,5-di-*tert*-butylbenzyl)amine,[22] and tris(pyridylmethyl)amine (tpa)[23] or the pentadentate bis(oxazoline)-based ligands (Scheme 5).[24] Fewer cases occur when the ligand is aromatic,[25] the same category to which compound **5** belongs.

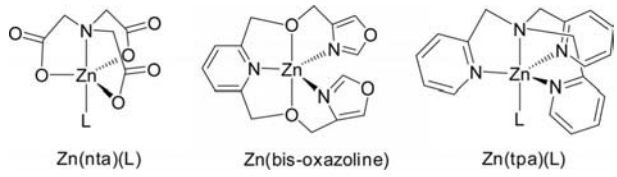

Scheme 5. Some Zn^{II} complexes with tripodal ligands forcing a trigonal-bipyramidal coordination mode.

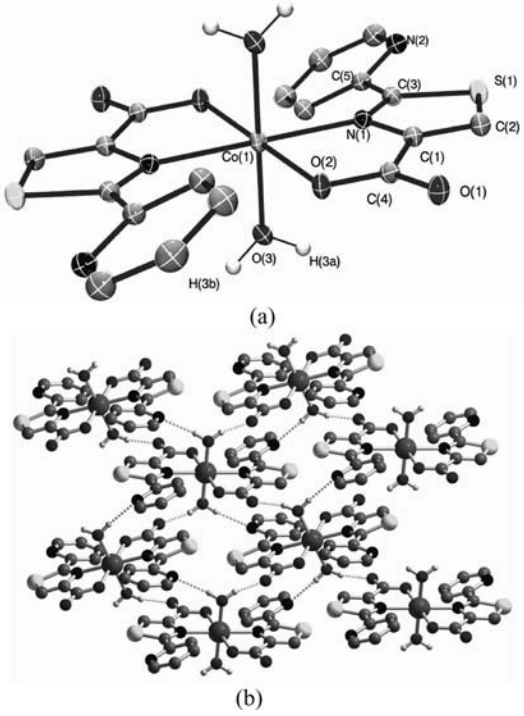

Figure 7. (a) Crystal structure of complex **6** and (b) its solid-state packing showing the hydrogen-bonding network. Hydrogen atoms on the organic ligands have been omitted for clarity. Thermal ellipsoids in (a) are drawn at the 40% probability level. Weak interactions are shown as yellow dotted lines.

The reaction of cobalt(II) acetate tetrahydrate with Htzc-py at pH 5 led to purple crystals of the complex $[Co(tzc\text{-}py)_2]\cdot 2H_2O$ (**6**). The coordination geometry around Co^{II} is octahedral (Figure 7, a) with the same ligand disposition as seen in **4** (Tables S13 and S14). The only difference is in the conformation of tzc-py⁻: The θ[N(1)–C(3)–C(5)–N(2)] dihedral angle is 161.3(3)° with a transoid N(1)–N(2) relative orientation identical to that of free Htzc-py.[6] The O(3)–H(3b)···O(1)# hydrogen bond between the aquo ligands and the carboxylic groups of neighboring molecules in the lattice is still present (Table 5). Finally, the N(pyridyl) engages in an additional O(3)–H(3a)···N(2)# hydrogen bond with the other proton on the aquo ligand (Figure 7, b). The *trans*-*N*,*N* disposition is probably the most energetically stable, nonetheless, when the N(pyridyl) atom is protonated (complex **4**), the (strongly stabilizing) intramolecular hydrogen bond balances the extra energy coming from a *trans*- to *cis*-*N*,*N* conformational change.

Table 5. Hydrogen bonds in **6**.

D–H···A[a]	*d*(D–H) [Å]	*d*(H···A) [Å]	*d*(D···A) [Å]	∠DHA [°]
O(3)–H(3b)···O(1)#2	0.86	1.82	2.660(3)	165.2
O(3)–H(3a)···N(2)#3	0.84	2.33	3.126(4)	159.5

[a] Symmetry transformations used to generate equivalent atoms; #2: $-x + 1$, $y + ½$, $-z + ½$; #3: x, $-y - ½$, $z - ½$.

Thermogravimetric Analysis and Variable-Temperature Powder X-ray Diffraction Analysis of the Isomeric Complexes $[Zn(x\text{-}tzc)_2]\cdot 2H_2O$ (x = 2, 4)

To collect additional characterization data for **1** and **2**, which contain two different isomeric forms (thiazole-4-carboxylate for **1** and thiazole-2-carboxylate for **2**) of the same ligand, a combined thermogravimetric analysis/variable-temperature PXRD experiment was carried out in the 30–450 °C temperature range. In **1** (Figure 8, a), coordinated water loss (10 wt.-%) occurs between 115 and 220 °C with the formation of a well-defined intermediate anhydrous $Zn(4\text{-}tzc)_2$ phase. Beyond 220 °C, decarboxylation and concomitant complex decomposition occurs with the appearance of the characteristic thiazole peak at m/z = 83 a.m.u. together with that of CO_2 (m/z = 44 a.m.u.) in the mass spectrum (Figure S3a). In **2**, the thermal behavior is very similar (see part b of Figure 8 and of Figure S3 in the Supporting Information), but the existence of the anhydrous species $Zn(2\text{-}tzc)_2$ is limited to a narrower tempera-

ture range (between 180 and 250 °C) because the decarboxylation of 2-Htzc occurs at lower temperatures than found for 4-Htzc (see above).

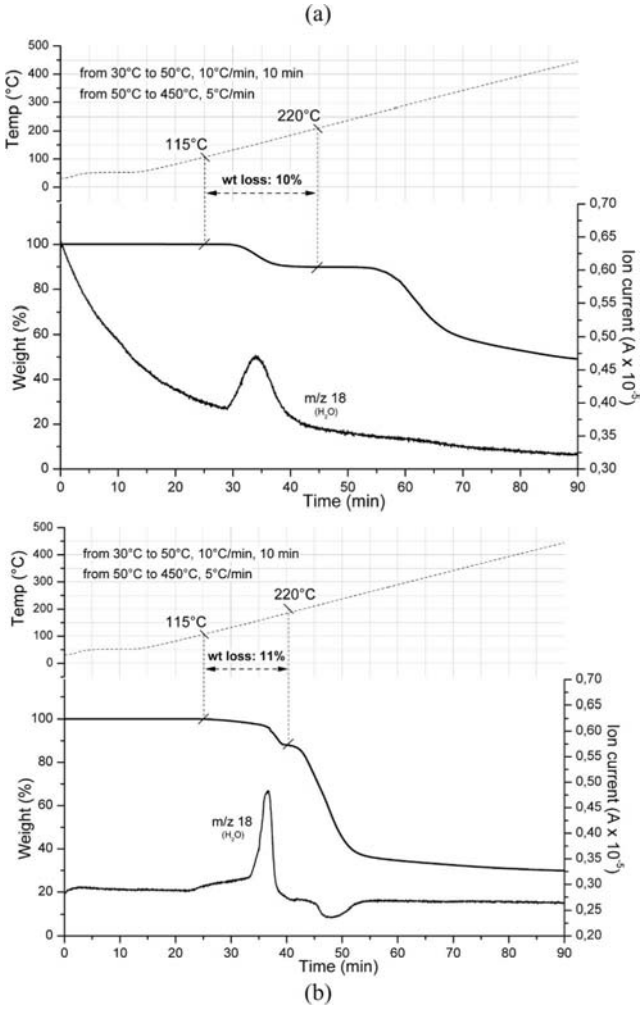

Figure 8. TG–MS spectra of complexes (a) **1** and (b) **2**.

The powder X-ray diffractograms of **1** recorded at different temperatures (Figure 9) mirror the results found in the TG–MS analysis: After the loss of aquo ligands, the peaks of the starting material disappear and reveal an amorphous phase above 150 °C. The anhydrous $Zn(4\text{-tzc})_2$ phase does not generate any kind of well-defined diffraction pattern, as may be expected if a change from an octahedral to (probably) tetrahedral coordination geometry is assumed when water is removed. The dramatic change in the coordination environment with temperature implies a structural lattice rearrangement that does not lead to a crystalline intermediate. Complete decomposition above 200 °C occurs, but no definite crystalline decomposition product could be detected in the PXRD profile.

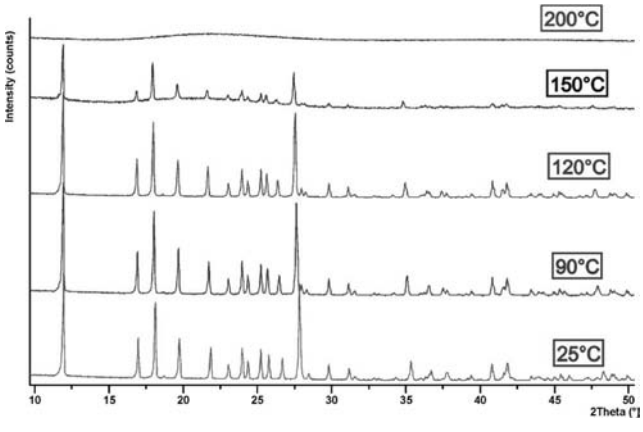

Figure 9. VT-PXRD spectra of **1**.

Conclusions

Novel coordination compounds containing thiazole-based ligands have been synthesized and characterized by IR spectroscopy and single-crystal X-ray diffraction analysis. Differences and analogies between the 2-Htzc/4-Htzc isomers have been identified. The influence of both pH and temperature on the solvothermal (hydrothermal) reactions has been carefully investigated. The coordination geometries of Zn^{II}, Co^{II}, and Cu^{II} in these species have been critically discussed and compared, with either octahedral or unusual trigonal-bipyramidal coordination geometries for zinc and cobalt, and square planar for copper. The presence of an extended hydrogen-bonding network due to the several polar groups in the asymmetric unit confers a "pseudo-polymeric" nature on these solids, being insoluble in all solvents. From this perspective, this study has to be considered as the first step towards the synthesis of thiazole-based metal–organic frameworks (MOFs) with potential applications in the field of gas storage. New polytopic ligands containing thiazole and oxazole rings are currently under investigation along with their reactivity with first-row transition-metal ions.

Experimental Section

General: Analytical grade reagents (including 4-Htzc) were obtained from Aldrich and used as received without further purification. Diethyl ether and acetonitrile solvents were dried and degassed by the MB SPS solvent purification system (http://www.solventpurifier.com/). Htzc-py[6] and $[Cu(MeCN)_4]PF_6$[26] were prepared according to literature procedures.

Thermal gravimetric analysis measurements were performed on an Exstar Thermo Gravimetric Analyzer (TG/DTA) Seiko 6200 under N_2 (50 mL/min) coupled with a ThermoStar™ GSD 301T (TGA–MS) instrument for MS gas analysis of volatiles. ^{1}H NMR spectra were recorded with Bruker Avance DRX 300 and DRX 400 spectrometers operating at 300.13 and 400.13 MHz, respectively. ^{13}C NMR spectra were recorded with the same instruments at 75.48 and 100.61 MHz, respectively. Chemical shifts (δ) are given in ppm relative to external tetramethylsilane and were calibrated against the residual protiated solvent (^{1}H) or the deuteriated solvent multiplet (^{13}C). Coupling constants (J) are reported in Hz. IR spectra (KBr pellets) were recorded with a Perkin–Elmer Spectrum BX Series FT-IR spectrometer in the range 4000–400 cm^{-1} with a 2 cm^{-1} resolution. Elemental analyses were performed using a Thermo FlashEA 1112 Series CHNSO elemental analyzer with an accepted tolerance of ±0.4 units.

X-ray data were collected either with an Enraf–Nonius CAD4 diffractometer equipped with a graphite monochromator (for **1** and **3**) or on an Oxford Diffraction XCALIBUR 3 diffractometer equipped with a CCD area detector (for all other compounds studied by X-ray diffraction techniques), in both cases using Mo-K_α radiation (λ = 0.7107 Å). The intensities collected in the first case were corrected for Lorentzian and polarization effects and their consistency checked every 2 h by collecting three standard reflections repeatedly. In the second case, the program used for the data collection was CrysAlis CCD 1.171.[27] Data reductions were carried out with the program CrysAlis RED 1.171[28] and the absorption corrections were applied with the program ABSPACK 1.17.[27] Direct methods implemented in SIR97[29] were used to solve the structures and the refinements were performed by full-matrix least-squares against F^2 implemented in SHELX97.[30] All the non-hydrogen atoms were refined anisotropically whereas the hydrogen atoms of the ligands were fixed in calculated positions and refined isotropically with the thermal factor depending on the atom to which they are bound. The hydrogen atoms on the coordinated water molecules in **1**, **2**, **4**, **5**, and **6** and on the protonated pyridyl ring of tzc-Hpy in **4** were found on the Fourier difference density maps and their positions were free to refine. Their thermal factors were related to the oxygen (or nitrogen) atom to which they are bound.

CCDC-781926 (for **1**), -781927 (for **2**), -781928 (for 2-Htzc), -781929 (for **3**), -781930 (for **4**), -781931 (for **5**), -781932 (for **6**), and 781933 [for $ZnCl_2$(κ-*N*-thiazole)$_2$] contain the supplementary crystallographic data for this paper. These data can be obtained free of charge from The Cambridge Crystallographic Data Centre via www.ccdc.cam.ac.uk/data_request/cif.

X-ray powder diffraction (XRPD) measurements were carried out with a Panalytical X'PERT PRO powder diffractometer equipped with a diffracted beam Ni filter and a PIXcel© solid-state detector in the 2θ = 5–75° region operating with Cu-K_α radiation (λ = 1.54 Å). Divergence of 0.25° and anti-scatter slits of 0.5° on the incident beam and a anti-scatter slit of 7.5 mm on the diffracted beam were used. The step-size was 0.0263° of 2θ with a counting time of 60 s per step. Variable-temperature (VT) X-ray powder diffractograms were collected in the 25–350 °C temperature range using a Anton Paar HTK 1200N Oven camera. The measurements were carried out at ambient pressure under a slow flow of N_2.

Synthesis of 2-Htzc: The original synthesis described in 1968 by Iversen[31] was slightly modified. A solution of freshly distilled 2-bromothiazole (9.00 g, 55 mmol) in diethyl ether (5 mL) was added quickly to a solution of *n*BuLi (1.6 M in hexanes, 38 mL, 60 mmol) in diethyl ether (100 mL) cooled to –78 °C. After stirring the mixture at low temperature for 10 min, gaseous CO_2 was bubbled into the reaction flask. A white solid immediately precipitated out. The bubbling was prolonged for 10 min and the mixture was stirred for another hour at –78 °C. Afterwards, slow warming to room temperature (1 h) was followed by quenching with H_2O (ca. 5 mL). The aqueous phase was washed with ethyl acetate (3 × 25 mL) and then acidified with concentrated HCl (pH 1, ca. 2 mL) to let the carboxylic acid gradually precipitate from the mother liquor. The off-white solid was collected by filtration through filter paper and washed several times with H_2O and Et_2O to afford pure 2-Htzc as a white crystalline solid; yield 4.562 g (64%). ^{1}H NMR (300.13 MHz, [D$_6$]DMSO, 25 °C): δ = 8.10 (d, $^3J_{H,H}$ = 3.0 Hz, 1 H), 8.08 (d, $^3J_{H,H}$ = 3.0 Hz, 1 H) ppm. ^{13}C{^{1}H}NMR (75.48 MHz, [D$_6$]DMSO, 25 °C): δ = 161.2, 159.5, 145.25, 127.14 ppm. IR (KBr): $\tilde{\nu}$ = 3140 (br, C–H) , 1719 (s, C=O) cm^{-1}. $C_4H_3NO_2S$ (129.14): calcd. C 37.20, H 2.34, N 10.85; found C 37.17, H 2.45, N 10.59.

Synthesis of [Zn(4-tzc)$_2$]·2H$_2$O (1): A two-fold excess of $Zn(ClO_4)_2$·6H_2O (1.73 g, 4.6 mmol) was dissolved with 4-Htzc (0.30 g, 2.3 mmol) in deionized water (10 mL). The clear solution was transferred to a Teflon®-lined stainless-steel autoclave, which was sealed and heated under autogenous pressure at 130 °C for 24 h. After slowly cooling overnight, colorless cube-like crystals of **1** were collected, washed with ethanol (4 × 10 mL), and dried under a stream of nitrogen at room temperature; yield 0.201 g (48%; calculated with respect to the ligand). ^{1}H NMR (400.13 MHz, [D$_6$]-DMSO, 25 °C): δ = 8.98 (s$_{app}$, 1 H), 8.12 (s$_{app}$, 1 H), 3.34 (s, H_2O) ppm. ^{13}C{^{1}H}NMR (100.61 MHz, [D$_6$]DMSO, 25 °C): δ = 162.69, 154.75, 152.83, 122.57 ppm. IR (KBr): $\tilde{\nu}$ = 3219 (br m, O–H), 3130 (m), 3114 (m, C–H), 1615 (vs, C=O) cm^{-1}. $C_8H_8N_2O_6S_2Zn$ (357.66): calcd. C 26.84, H 2.23, N 7.83; found C 26.92, H 2.05, N 7.82.

Synthesis of [Zn(2-tzc)$_2$]·2H$_2$O (2): $Zn(OAc)_2$·2H_2O (1.36 g, 6.2 mmol) was dissolved with 2-Htzc (0.40 g, 3.1 mmol) in deionized water (5 mL). The clear solution was transferred to a Teflon®-lined stainless-steel autoclave, which was sealed and heated under autogenous pressure at 90 °C for 24 h. After slowly cooling overnight, colorless prismatic crystals of **2** were collected, washed with ethanol (4 × 10 mL), and dried under a stream of nitrogen at room temperature; yield 0.291 g (55%; calculated with respect to the ligand). ^{1}H NMR (400 MHz, [D$_6$]DMSO, 25 °C): δ = 7.99 (d, $^3J_{H,H}$ = 3.1 Hz, 1 H), 8.08 (d, $^3J_{H,H}$ = 3.0 Hz, 1 H), 3.34 (s, H_2O) ppm. ^{13}C{^{1}H} NMR (100.6 MHz, [D$_6$]DMSO, 25 °C): δ = 168.69, 160.43, 140.01, 126.74 ppm. IR (KBr): $\tilde{\nu}$ = 3269 (s, br, O–H), 3115 (s), 3090 (s, C–H), 1676 (vs, C=O) cm^{-1}. $C_8H_8N_2O_6S_2Zn$ (357.66): calcd. C 26.84, H 2.23, N 7.83; found C 26.80, H 2.21, N 7.80.

Synthesis of [Cu(4-tzc)$_2$] (3):[32] Tetrakis(acetonitrile)copper(I) hexafluorophosphate $[Cu(MeCN)_4]PF_6$ (0.54 g, 1.1 mmol) was dissolved with 4-Htzc (0.30 g, 2.3 mmol) in acetonitrile (8 mL). The clear solution was transferred to a Teflon®-lined stainless-steel autoclave, which was sealed and heated under autogenous pressure at 110 °C for 24 h. After slowly cooling overnight, blue crystals of **3** were collected, washed with ethanol (4 × 10 mL), and dried under a stream of nitrogen at room temperature; yield 0.102 g (27%; calculated with respect to the ligand). IR (KBr): $\tilde{\nu}$ = 3094 (s, C–H), 1634 (vs, C=O) cm^{-1}. $C_8H_4CuN_2O_4S_2$ (318.80): calcd. C 30.05, H 1.26, N 8.76; found C 29.97, H 1.15, N 8.44.

Synthesis of [Zn(tzc-Hpy)$_2$·2H$_2$O](ClO$_4$)$_2$ (4): $Zn(ClO_4)_2$·6H_2O (1.08 g, 2.9 mmol) was dissolved with Htzc-py (0.30 g, 1.45 mmol) in deionized water (5 mL). The clear solution was transferred to a Teflon®-lined stainless-steel autoclave, which was sealed and heated under autogenous pressure at 130 °C for 24 h. After slowly cooling overnight, colorless crystals of **4** were collected, washed with ethanol (4 × 10 mL), and dried under a stream of nitrogen at room temperature; yield 0.387 g (75%; calculated with respect to the ligand). ^{1}H NMR (400 MHz, [D$_6$]DMSO, 25 °C): δ = 8.65 (d$_{app}$, J = 4.8, Hz, 1 H), 8.56 (s, 1 H), 8.14 (d$_{app}$, J = 7.7 Hz, 1 H), 8.00 (dt$_{app}$, J = 7.7, 1.5 Hz, 1 H), 7.54 (ddd, J = 7.7, 4.8, 0.8 Hz, 1 H), 3.75 (br. s, 1 H) ppm. ^{13}C{^{1}H} NMR (100.61 MHz, [D$_6$]DMSO, 25 °C): δ = 168.8, 162.1, 149.9, 149.8, 148.5, 138.1, 130.8, 125.7, 119.5 ppm. IR (KBr): $\tilde{\nu}$ = 3524 (m, O–H), 3112 (m), 3091 (m), 3058 (w, C–H) , 2536 (br w, N–H) , 1697 (m), 1596 (m, C=O) cm^{-1}. $C_{18}H_{16}Cl_2N_4O_{14}S_2Zn$ (712.75): calcd. C 30.33, H 2.26, N 7.86; found C 30.14, H 2.29, N 7.65.

Synthesis of [Zn(tzc-py)$_2$]·H$_2$O (5): $Zn(OAc)_2$·2H_2O (0.64 g, 2.9 mmol) was dissolved with Htzc-py (0.30 g, 1.45 mmol) in deionized water (5 mL). The clear solution was transferred to a Teflon®-lined stainless-steel autoclave, which was sealed and heated under autogenous pressure at 130 °C for 24 h. After slowly cooling over-

night, colorless crystals of **5** were collected, washed with ethanol (4 × 10 mL), and dried under a stream of nitrogen at room temperature; yield 0.080 g (22%; calculated with respect to the ligand). ^{1}H NMR (400.13 MHz, [D$_6$]DMSO, 25 °C): δ = 8.62 (d$_{app}$, J = 4.5 Hz, 1 H), 8.48 (d$_{app}$, J = 7.1 Hz, 1 H), 8.23 (s, 1 H), 8.00 (t$_{app}$, J = 7.1 Hz, 1 H), 7.51 (dd, J = 7.1, 4.5 Hz, 1 H), 3.33 (s, H_2O) ppm. ^{13}C{^{1}H} NMR (100.6 MHz, [D$_6$]DMSO, 25 °C): δ = 168.5, 164.0, 153.4, 149.6, 179.0, 137.7, 126.1, 125.6, 120.4 ppm. IR (KBr): $\tilde{\nu}$ = 3425 (br w, O–H), 3130 (w), 3089 (m, C–H) , 1654 (vs), 1609 (vs, C=O) cm^{-1}. $C_{18}H_{12}N_4O_5S_2Zn$ (493.85): calcd. C 43.78, H 2.45, N 11.34; found C 43.16, H 2.32, N 11.62.

Synthesis of [Co(tzc-py)$_2$]·2H$_2$O (6):[32] $Co(OAc)_2{\cdot}4H_2O$ (0.72 g, 2.9 mmol) was dissolved with Htzc-py (0.30 g, 1.45 mmol) in deionized water (5 mL). The clear solution was transferred to a Teflon®-lined stainless-steel autoclave, which was sealed and heated under autogenous pressure at 130 °C for 24 h. After slowly cooling overnight, hexagonal light-yellow crystals of **6** were collected, washed with ethanol (4 × 10 mL), and dried under a stream of nitrogen at room temperature; yield 0.190 g (52%; calculated with respect to the ligand). IR (KBr): $\tilde{\nu}$ = 3428 (m, O–H), 3140 (s), 3060 (w, C–H), 1609 (vs, C=O) cm^{-1}. $C_{18}H_{14}CoN_4O_6S_2$ (505.39): calcd. C 42.78, H 2.79, N 11.09; found C 42.65, H 2.70, N 11.22.

Supporting Information (see footnote on the first page of this article): Crystal data and structure refinement plus tables reporting selected bond lengths and angles for 2-Htzc, complexes **1**–**6**, and $ZnCl_2$(κ-*N*-thiazole)$_2$. TG–MS plots for 2-Htzc, 4-Htzc, Htzc-py and ambient-temperature PXRD spectra of compounds **1**–**6**.

Acknowledgments

Ente Cassa di Risparmio di Firenze (ECRF) through the project FIRENZE HYDROLAB (http://www.iccom.cnr.it/hydrolab) is kindly acknowledged for a post-doctoral grant to A. R. and a doctoral grant to B. D. C. Thanks are also expressed to the Ministero dell'Università e della Ricerca (MIUR) for financial support through the PRIN 2007 project. A. R. would also like to thank Dr. Andrea Ienco and Dr. Werner Oberhauser at ICCOM-CNR for help with the variable-temperature PXRD measurements. Dr. Annalisa Guerri at the Centre of Structural Crystallography of the University of Florence (http://www.crist.unifi.it/) is also acknowledged for fruitful discussions on crystallography.

[1] a) J. Hasegawa, M. Higuchi, Y. Hijikata, S. Kitagawa, *Chem. Mater.* **2009**, *21*, 1829–1833; b) R. Vaidhyanathan, S. S. Iremonger, K. W. Dawson, G. K. H. Shimizu, *Chem. Commun.* **2009**, 5230–5232; c) H. Furukawa, O. M. Yaghi, *J. Am. Chem. Soc.* **2009**, *131*, 8875–8883; d) A. P. Nelson, O. K. Farha, K. L. Mulfort, J. T. Hupp, *J. Am. Chem. Soc.* **2009**, *131*, 458–460; e) H. J. Choi, M. Dincă, J. R. Long, *J. Am. Chem. Soc.* **2008**, *130*, 7848–7850; f) S. S. Han, H. Furukawa, O. M. Yaghi, W. A. Goddard III, *J. Am. Chem. Soc.* **2008**, *130*, 11580–11581; g) J. R. Hunt, C. J. Doonan, J. D. LeVangie, A. P. Côté, O. M. Yaghi, *J. Am. Chem. Soc.* **2008**, *130*, 11872–11873; h) S. R. Miller, G. M. Pearce, P. A. Wright, F. Bonino, S. Chavan, S. Bordiga, I. Margiolaki, N. Guillou, G. Férey, S. Bourrelly, P. L. Llewellyn, *J. Am. Chem. Soc.* **2008**, *130*, 15967–15981; i) J. G. Vitillo, L. Regli, S. Chavan, G. Ricchiardi, G. Spoto, P. D. C. Dietzel, S. Bordiga, A. Zecchina, *J. Am. Chem. Soc.* **2008**, *130*, 8386–8396; j) P. D. C. Dietzel, R. E. Johnsen, H. Fjellvag, S. Bordiga, E. Groppo, S. Chavan, R. Blom, *Chem. Commun.* **2008**, 5125–5127; k) A. Rossin, A. Ienco, F. Costantino, T. Montini, B. Di Credico, M. Caporali, L. Gonsalvi, P. Fornasiero, M. Peruzzini, *Cryst. Growth Des.* **2008**, *8*, 3302–3308.

[2] For general recent reviews, see: a) M. Nishio, Y. Umezawa, K. Honda, S. Tsuboyama, H. Suezawa, *CrystEngComm* **2009**, *11*, 1757–1788, and references cited therein; b) I. A. Baburin, V. A. Blatov, L. Carlucci, G. Ciani, D. M. Proserpio, *CrystEngComm* **2008**, *10*, 1822–1838, and references cited therein.

[3] For general texts, see: a) J. A. Joule, K. Mills, *Heterocyclic Chemistry*, 5th ed., Wiley, Chichester, **2010**; b) J. V. Metzger, in: *Comprehensive Heterocyclic Chemistry*, Pergamon Press, Oxford, **1984**.

[4] a) I. Boldog, J.-C. Daran, A. N. Chernega, E. B. Rusanov, H. Krautscheid, K. V. Domasevitch, *Cryst. Growth Des.* **2009**, *9*, 2895–2905; b) J.-G. Trujillo-Ferrara, I. I. Padilla-Martinez, F. J. Martinez-Martinez, H. Hoepfl, N. Farfan-Garcia, E. V. Garcia-Baez, *Acta Crystallogr., Sect. C* **2004**, *60*, o723–o726; c) A. Cammers, S. Parkin, *CrystEngComm* **2004**, *6*, 168–172; d) D. E. Lynch, I. McClenaghan, M. E. Light, S. J. Coles, *Cryst. Eng.* **2002**, *5*, 123–136.

[5] a) A. Aijaz, E. Barea, P. K. Bharadwaj, *Cryst. Growth Des.* **2009**, *9*, 4480–4486; b) J.-D. Lin, J.-W. Cheng, S.-W. Du, *Cryst. Growth Des.* **2008**, *8*, 3345–3353; c) A. Mukhopadhyay, S. Pal, *Eur. J. Inorg. Chem.* **2006**, 4879–4887.

[6] B. Di Credico, G. Reginato, L. Gonsalvi, M. Peruzzini, A. Rossin, *Tetrahedron* **2011**, *67*, 267–274.

[7] a) K. T. Prasad, B. Therrien, K. M. Rao, *J. Organomet. Chem.* **2010**, *695*, 226–234; b) A. Aprea, V. Colombo, S. Galli, N. Masciocchi, A. Maspero, G. Palmisano, *Solid State Sci.* **2010**, *12*, 795–802; c) K. A. Siddiqui, G. K. Mehrotra, R. L. La Duca, *Polyhedron* **2009**, *28*, 4077–4083; d) X.-D. Chen, H.-F. Wu, X.-H. Zhao, X.-J. Zhao, M. Du, *Cryst. Growth Des.* **2007**, *7*, 124–131; e) J. M. Ellsworth, C.-Y. Su, Z. Khaliq, R. E. Hipp, A. M. Goforth, M. D. Smith, H.-C. zur Loye, *J. Mol. Struct.* **2006**, *796*, 86–94; f) C.-Y. Su, M. D. Smith, A. M. Goforth, H.-C. zur Loye, *Inorg. Chem.* **2004**, *43*, 6881–6883; g) H.-D. Yin, C.-H. Wang, *Appl. Organomet. Chem.* **2004**, *18*, 411–412.

[8] a) X.-Y. Wang, S. C. Sevov, *Chem. Mater.* **2007**, *19*, 4906–4912; b) S. A. Darlymple, G. K. H. Shimizu, *J. Am. Chem. Soc.* **2007**, *129*, 12114–12116.

[9] For the reactivity of substituted thiazoles, see: a) G. W. Gibble, J. A. Joule, *Progress in Heterocyclic Chemistry*, Elsevier, Oxford, **2009**, vol. 20; b) J. V. Metzger, *Thiazole and its Derivatives*, Wiley, New York, **1979**, and references cited therein.

[10] Symmetry transformation used (#) = $-x$, $y + ½$, $-z + 2$.

[11] K. Byrappa, M. Yoshimura, *Handbook of Hydrothermal Technology: a technology for crystal growth and materials processing*, Noyes Publications, Norwich, New York, USA, **2001**.

[12] a) A. Y. Robin, K. M. Fromm, *Coord. Chem. Rev.* **2006**, *250*, 2127–2157; b) O. M. Yaghi, M. O'Keeffe, N. W. Ockwig, H. K. Chae, M. Eddaoudi, J. Kim, *Nature* **2003**, *423*, 705–714; c) B. Moulton, M. J. Zaworotko, *Chem. Rev.* **2001**, *101*, 1629–1658; d) D. Braga, F. Grepioni, G. R. Desiraju, *Chem. Rev.* **1998**, *98*, 1375–1405; e) O. M. Yaghi, H. Li, C. Davis, D. Richardson, T. L. Groy, *Acc. Chem. Res.* **1998**, *31*, 474–484.

[13] a) C. Nather, G. Bhosekar, I. Jess, *Inorg. Chem.* **2007**, *46*, 8079–8087; b) P. M. Forster, N. Stock, A. K. Cheetham, *Angew. Chem. Int. Ed.* **2005**, *44*, 7608–7611; c) N. Stock, T. Bein, *J. Mater. Chem.* **2005**, *15*, 1384–1391; d) P. M. Forster, A. R. Burbank, C. Livage, G. Férey, A. K. Cheetham, *Chem. Commun.* **2004**, 368–369.

[14] This compound was synthesized and characterized spectroscopically in 1970, but its crystal structure has never been reported to date: M. N. Hughes, K. J. Rutt, *J. Chem. Soc. A* **1970**, 3015–3019.

[15] G. Ferguson, C. Glidewell, *Acta Crystallogr., Sect. E* **2003**, *59*, m710–m712.

[16] Y.-Y. Liu, *J. Coord. Chem.* **2007**, *60*, 2597–2605.

[17] M. Gryz, W. Starosta, J. Leciejewicz, *J. Coord. Chem.* **2007**, *60*, 539–546.

[18] a) X.-F. Lin, *Acta Crystallogr., Sect. E* **2006**, *62*, m2039–m2040; b) J.-W. Liu, S. Gao, L.-H. Huo, C.-S. Gu, H. Zhao, J.-G. Zhao, *Acta Crystallogr., Sect. E* **2004**, *60*, m1697–m1699.

[19] B.-X. Liu, J.-Y. Yu, D.-J. Xu, *Acta Crystallogr., Sect. E* **2006**, *62*, m67–m68.
[20] See also: Y.-R. Zhong, M.-L. Cao, H.-Y. Mo, B.-H. Ye, *Cryst. Growth Des.* **2008**, *8*, 2282–2290.
[21] R. Puchta, N. van Eikema Hommes, R. Meier, R. van Eldik, *Dalton Trans.* **2006**, 3392–3395.
[22] A. Abufarag, H. Vahrenkamp, *Inorg. Chem.* **1995**, *34*, 3279–3284.
[23] J. W. Canary, C. S. Allen, J. M. Castagnetto, Y. Wang, *J. Am. Chem. Soc.* **1995**, *117*, 8484–8485.
[24] M. Seitz, S. Stempfhuber, M. Zabel, M. Schütz, O. Reiser, *Angew. Chem. Int. Ed.* **2005**, *44*, 242–245.
[25] a) T. Yamada, H. Kitagawa, *J. Am. Chem. Soc.* **2009**, *131*, 6312–6313; b) C. Kirchner, B. Krebs, *Inorg. Chem.* **1987**, *26*, 3569–3576.
[26] R. D. Stephens, *Inorg. Synth.* **1979**, *19*, 90–93.
[27] *CrysAlis CCD 1.171.31.2*, *CrysAlis171.NET*, Oxford Diffraction Ltd., **2006**.
[28] *CrysAlis RED 1.171.31.2*, *CrysAlis171.NET*, Oxford Diffraction Ltd., **2006**.
[29] A. Altomare, M. C. Burla, M. Camalli, G. L. Cascarano, C. Giacovazzo, A. Guagliardi, A. G. G. Moliterni, G. Polidori, R. Spagna, *J. Appl. Crystallogr.* **1999**, *32*, 115.
[30] G. M. Sheldrick, *SHELXL97*, University of Göttingen, Göttingen, **1997**.
[31] P. E. Iversen, *Acta Chem. Scand.* **1968**, *22*, 694–695.
[32] Owing to their complete insolubility in common NMR solvents, solution NMR spectroscopic data for compounds **3** and **6** could not be recorded.

Received: August 30, 2010
Published Online: December 22, 2010

